

Thermally stimulated discharge current (TSDC) characteristics in β -phase PVDF–BaTiO₃ nanocomposites

M. S. Gaur · Pramod Kumar Singh ·
Asif Ali · Rekha Singh

Received: 6 November 2013 / Accepted: 3 June 2014 / Published online: 20 July 2014
© Akadémiai Kiadó, Budapest, Hungary 2014

Abstract β -phase polyvinylidene fluoride (PVDF)–BaTiO₃ nanocomposite samples have been prepared by solution mixing method. XRD data represent that the crystallinity of PVDF decreases with increase in loading level of BaTiO₃ nanoparticles. DSC curve represents that the melting point of PVDF is lightly affected by loading concentration of BaTiO₃. The morphology and microstructure of PVDF and PVDF embedded by BaTiO₃ nanofillers were investigated by using inverted contrast microscopy (ICM) and scanning electron microscopy (SEM). FTIR interferometry is proven that PVDF and BaTiO₃ are not chemically interacting; therefore, interaction of BaTiO₃ is van der Waals type of interaction. The thermally stimulated discharge current (TSDC) of PVDF and PVDF–BaTiO₃ nanocomposites sample was characterized by single peak. The observed TSDC peak is discussed on the basis of dipolar and interfacial polarization.

Keywords PVDF · BaTiO₃ · Structural analysis · FTIR · XRD · TSDC

Introduction

The polymer nanostructured materials or polymer nanocomposites represent the alternative of conventional polymers and polymer blends. Nanocomposites are formed when discrete

constituents on the order of a few nanometers are incorporated in the polymer matrix [1, 2]. In past few decades, the utility of inorganic nanoparticles in polymer matrix as additives to enhance polymer performance has been established and now provide numerous industrial applications [3]. The piezoelectric polyvinylidene fluoride (PVDF) and its copolymers are widely applied materials in both actuation and sensing mechanisms. In these nanocomposites, the final properties depend essentially on parameters such as grain size of particle, method of preparation of composites, and on the dispersion of the ceramic particles into the polymer matrix [4–7]. Piezoelectric ceramic materials have been under investigation for their active responses and their effective use in sensor and actuator applications [8]. Nanocomposites of electroactive ceramics and a ferroelectric polymer are very attractive for many applications as their properties can be easily tailored to suit particular performance requirements [9–14]. The piezoelectric and pyroelectric properties of PVDF have led for important technological applications. Piezoelectric polymers have advantage over piezoelectric ceramics because of light weight and excellent polarization properties [15–17]. Therefore, piezoelectric polymer (PVDF) is more useful for industrial as well as medical application. Despite advantageous mechanical properties such as flexibility and reasonable strength, it has excellent piezoelectric response [18]. Although, there are several techniques to understand structural dynamics in polymer nanocomposites, however, X-ray diffraction (XRD), scanning electron microscopy (SEM), and optical microscopy techniques are very useful tool to investigate the structural morphology of polymer nanocomposites material [19–21], whereas differential thermal analysis (DTA) and differential scanning calorimetry (DSC) provide the thermal behavior of polymer nanocomposites.

Bucci and Fieschi et al. proposed the method of thermally stimulated depolarization/discharge current (TSDC)

M. S. Gaur (✉) · P. K. Singh · A. Ali · R. Singh
Department of Physics, Hindustan College of Science &
Technology, Farah, Mathura, U.P., India
e-mail: mulayamgaur@rediffmail.com

M. S. Gaur · P. K. Singh · A. Ali · R. Singh
Uttar Pradesh Technical University, Lucknow, U.P., India

for the insulating polymers [22]. TSDC has become a widely used experimental technique for the investigation of various insulating material parameters such as charge storage, charge decay process, thermal stability, activation energy, and relaxation process [23]. TSDC studies on polymer has been shown that the total charge storage in polymeric material and various mechanism, which contribute the charge storage and transport process during the charging and discharging of polymers [24–29].

DTA can be used to study the melting point, polymorphism, thermal stability of the compound and comparison of the structure of the compounds can be studied. The DTA signal is the temperature difference between sample and reference, typically plotted against temperature. DSC is very similar to DTA, but due to a more sophisticated construction not only temperature itself, but additionally the heat flow into (or from) the sample can be measured. This allows, in addition to temperature, also measuring the heat energy (e.g., heat of fusion) that is consumed by the sample. TSDC is important to study the thermo-electrical properties of material under polarization and depolarization mode.

Although there have been several reports [30, 31] on PVDF/BaTiO₃ nanocomposites with high loading of BaTiO₃ (up to 50 mass% by volume), however, low loading concentration of BaTiO₃ is not much reported in the literature. The β -phase PVDF shows the good piezoelectric coefficient due to net dipole moment present in material, therefore, β -phase is the most important in so many applications [32]. There are so many crystal phases are present in polymeric samples; the crystal phase morphology of PVDF films is verified by various methods like Fourier transform infrared spectroscopy (FTIR) and XRD to ensure the β -phase [33]. In the present work, we will study the effect of low loading concentration (i.e. 2, 4, 6 and 8 mass%) of BaTiO₃ on β -phase PVDF. Structural morphology and thermo-electrical properties are investigated by using XRD, SEM, FTIR, DSC, DTA, and TSDC techniques. These experiments will provide the valuable information about the molecular interactions in PVDF and PVDF–BaTiO₃ nanocomposite samples. The main objective of this work was to understand the polarization–depolarization mechanism as well as change in structural morphology of PVDF/PVDF–BaTiO₃ samples. The outcome of TSDC will be correlated with nature of d_{33} coefficient. This is an attempt to develop the correlation of TSDC as a main experiment with other experimental techniques.

Experimental

Material

β -phase PVDF and BaTiO₃ nanoparticle (cubic crystalline phase) of size less than 100 nm and with purity $\geq 99\%$

trace metal basis were procured by Sigma Aldrich. The dielectric constant of BaTiO₃ is 5,379 at 100 Hz. All the samples of Pristine (PVDF) and BaTiO₃ filled PVDF nanocomposite samples were prepared by using the solution grown technique. The analytical grade N–N Dimethylformamide (DMF) used as a solvent was procured from Merck India Ltd., New Delhi, India.

Sample preparation

The thin sample of PVDF and PVDF + BaTiO₃ was prepared. The 10-g amount of PVDF powder dissolved in a glass beaker containing 100 mL of N,N-dimethylformamide (DMF) solvent, then the solution of PVDF/DMF was kept onto magnetic stirrer for 5 h at 333 K. The BaTiO₃ nanocomposite powders 5 mass% of PVDF were dissolved in 20 mL DMF in separate glass beaker, then the solutions of BaTiO₃ nanoparticles were kept onto magnetic stirred at simultaneous conditions of PVDF/DMF solution. Then the solution of BaTiO₃ nanoparticles mixed drop by drop in the solution of PVDF/DMF. Then the solution of PVDF/BaTiO₃ nanocomposite was kept onto stirred for 24 h. Solutions were seen at regular intervals to check the viscosity. After that the solution was sonicated for 15 min at ultrasonic frequency for the homogenous and better dispersion of BaTiO₃ nanoparticles into PVDF with the help of sonicator. Now, final solution was poured onto glass substrates. The solvent was then allowed to evaporate inside an oven at room temperature for 24 h to yield the desired samples. The nanocomposite samples in the form of film were easily peeled off from glass substrates. The dried films of nanocomposites were subjected to room temperature to outgas at a vacuum of 10^{-5} Torr for a further period of 24 h to remove the residual solvent. The films were aluminized over the central circular area of diameter 3.5 cm using high vacuum coating unit.

Characterization

The XRD patterns of β -phase polyvinylidene fluoride (PVDF)/BaTiO₃ nanocomposite have been recorded at room temperature using diffractometer with Cu K α ($\lambda = 1.5405 \text{ \AA}$) radiation in θ – θ locked couple mode from the Bruker AXS D8 diffractometer with scan speed of 1° min^{-1} . The diffraction angle (2θ) has been varied from 5° to 80° with a step size of 0.02. The measurements were done under ambient pressure conditions at room temperature. Each experiment was repeated at least twice and with both faces of the samples alternatively exposed to the X-rays to check the reproducibility.

The surface morphology of the β -phase (PVDF)/BaTiO₃ nanocomposite was obtained using the SEM (LEO 435 VP) and inverted contrast microscopy (ICM). The film surfaces

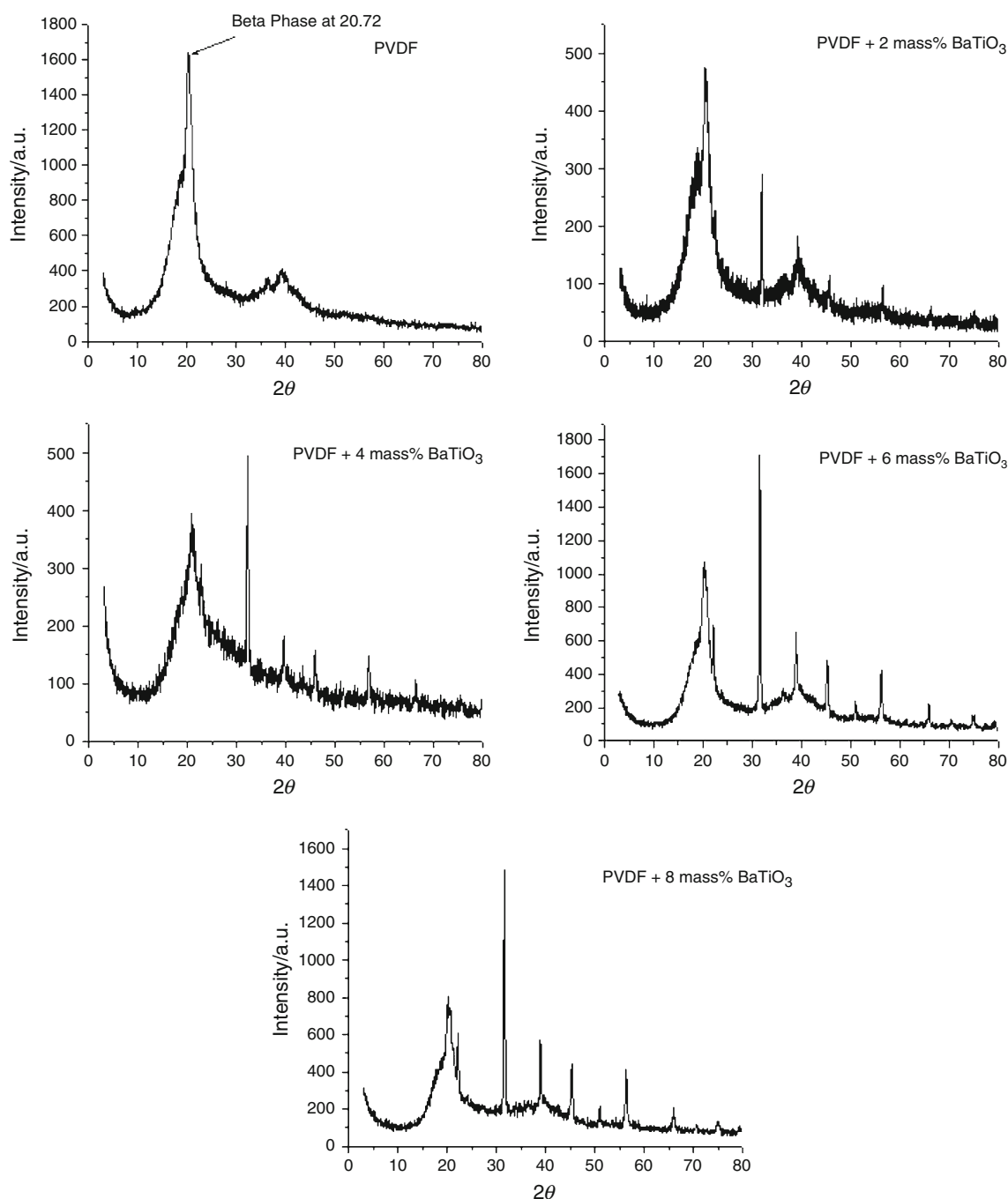


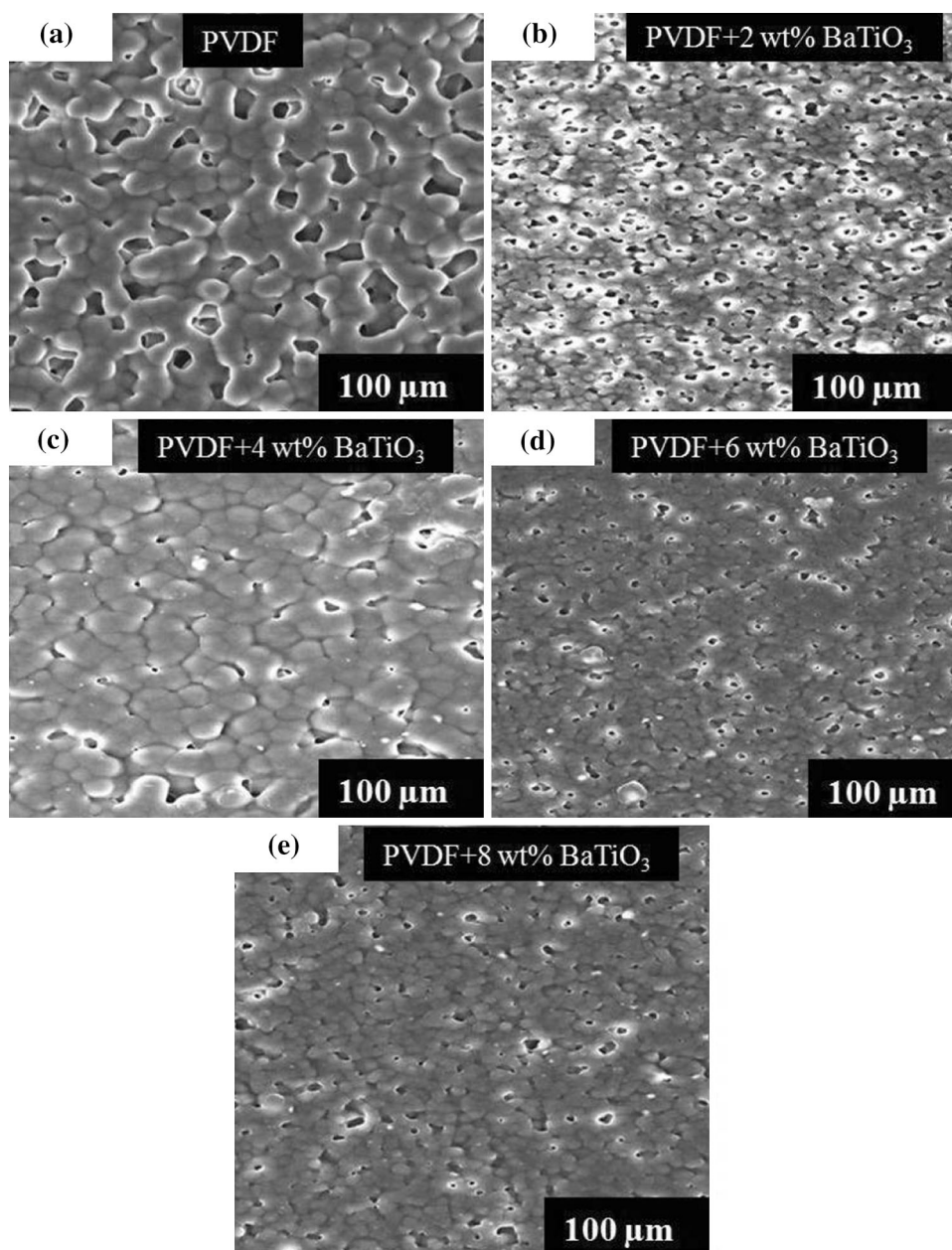
Fig. 1 X-ray Diffraction spectra of β phase PVDF and PVDF + BaTiO₃ nanocomposite

were gold coated prior to being scanned under high resolution scanning microscope.

DSC and DTA were performed on a Perkin Elmer (Pyris Diamond) instrument in nitrogen environment (200 mL min^{-1}) to record the thermal stability of β -phase PVDF nanocomposite samples. The samples were heated with the heating rate of $10 \text{ }^\circ\text{C min}^{-1}$ from 30 to $300 \text{ }^\circ\text{C}$. The weight loss and thermal decomposition temperature were measured and reported as a function of temperature.

The samples were thermally poled at room temperature with different polarizing field (i.e., 10 , 20 , 30 , 40 kV cm^{-1}). The aluminum electrode was vacuum aluminized by vacuum coating unit. The total time of polarization was taken to be 2.5 h including cooling of samples under electrical stress. The TSDC was measured by means of Keithley electrometer (Model no. 6514) connected in external circuit with constant heating rate of $3 \text{ }^\circ\text{C min}^{-1}$. In order to understand the surface morphology of polymers

Fig. 2 Scanning electron micrograph of β phase PVDF and PVDF + BaTiO₃ nanocomposites



and polymer nanocomposite samples, the micrograph of PVDF and PVDF–BaTiO₃ samples was recorded by optical micrograph (Nikon ECILTSE, Model No. PE2000). The d_{33} coefficients of PVDF and PVDF–BaTiO₃ samples were measured by piezo tech (PM 100) piezometer at 110 Hz frequency.

Results and discussion

XRD analysis

XRD studies have been carried out in order to monitor the formation of the nanocomposites. XRD analysis of β -phase

PVDF and nanocomposites (i.e., β -phase PVDF + BaTiO₃) have been taken with different mass% of BaTiO₃. XRD analysis used to study the structural change in crystalline behavior of PVDF nanocomposites with the incorporation of BaTiO₃ in PVDF matrix. XRD spectra of pristine β -phase PVDF and nanocomposites have been shown in Fig. 1. Pristine PVDF spectra are showing the one sharp peak at 20.72° and one more peak at 40° as shown in XRD spectra of pristine PVDF, a sharp peak around 20.7, which corresponding to β -phase as reported in the literature [34], whereas β -phase PVDF nanocomposites spectra are showing some more sharp peaks at different value of 2θ . XRD result showing the full width half maxima (FWHM) increases with the decreasing the crystallite size along with the increasing

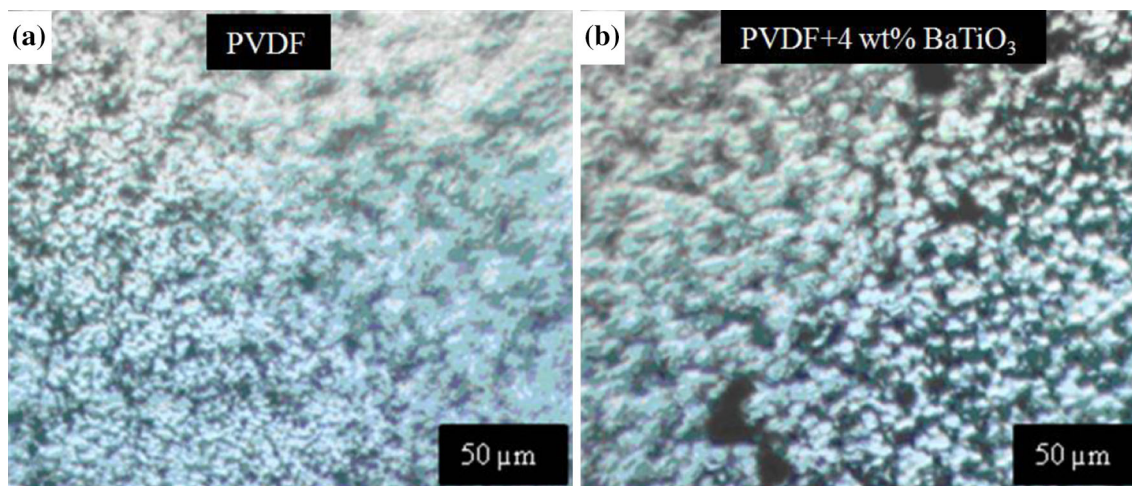


Fig. 3 Optical micrographs (a), PVDF (b). PVDF + 4 mass% BaTiO₃ nanocomposite

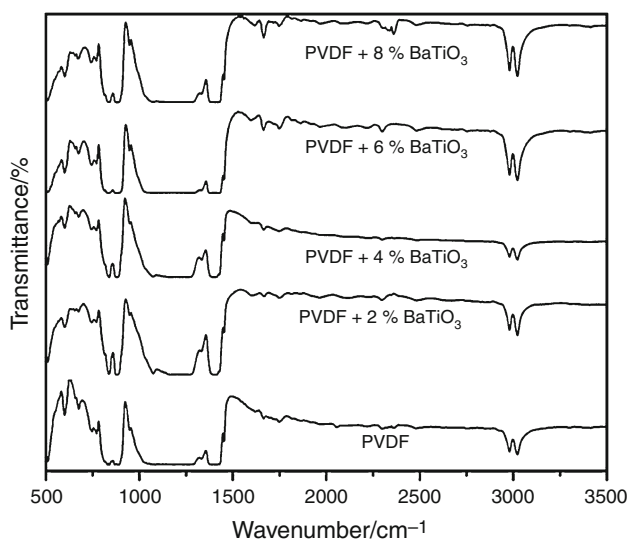


Fig. 4 FTIR spectroscopy spectra of phase PVDF and PVDF + BaTiO₃ nanocomposites

concentration of nanofillers till 4 mass%, after 4 mass% crystallite size increases. The observed increase in peak intensity and FWHM is generally associated with decrease in crystallite size of the polymer nanocomposite. The crystallite size and width of the peak have been related by Scherer formula [35], the average crystallite size *L* has been calculated by Scherer formula

$$L = \frac{k\lambda}{\beta \cos \theta} \tag{1}$$

where β is the FWHM of the peak (in radian) and *k* is the shape factor whose value is equal to 0.9. The $k = 0.9$ in the above equation, the crystallite size of β-phase pristine PVDF and BaTiO₃ filled β-phase PVDF nanocomposites samples were calculated. The crystallite size is decreasing

Table 1 FTIR analysis of β phase PVDF and PVDF + BaTiO₃ nanocomposites

Wave number/cm ⁻¹	Source of origin
598.31(s)	CF ₂ bending and skeletal
674.15(w)	CF ₂ rocking
743.13(w)	CF ₂ rocking
771.53(w)	CF ₂ rocking
836.45(s)	CH ₂ out of plane wagging
881.08(s)	CH ₂ rocking vibrations
946.00(w)	CH ₂ beading
1403.55(s)	CH ₂ Scissoring
1452.55(w)	CH ₂ /Ti–O Scissoring/vibrations
1664.16(s)	C=C bond vibrates
1748.43(s)	C=O stretching

Here, *s* means strong bond and *w* means weak bond

after loading of BaTiO₃ nanoparticles with different concentration in β-phase PVDF. Scherer has also showed that crystallite size *L* is inversely proportional to FWHM (β). The degree of % crystallinity of polymer nanocomposites samples has been calculated using the following relation [36]:

$$K = \frac{A}{A'} \times 100 \% \tag{2}$$

where *A* is the total area of the peaks (area of crystalline and amorphous peaks) and *A'* is the total area under the diffraction pattern. We found that as we increase the concentration of BaTiO₃ nanofillers in β-phase PVDF, the percentage crystallinity of the nanocomposites has been decreases with decreasing intensity of the main peak up to 4 mass% loading concentration, then % crystallinity increasing with intensity, and again it decreases at 8 mass%

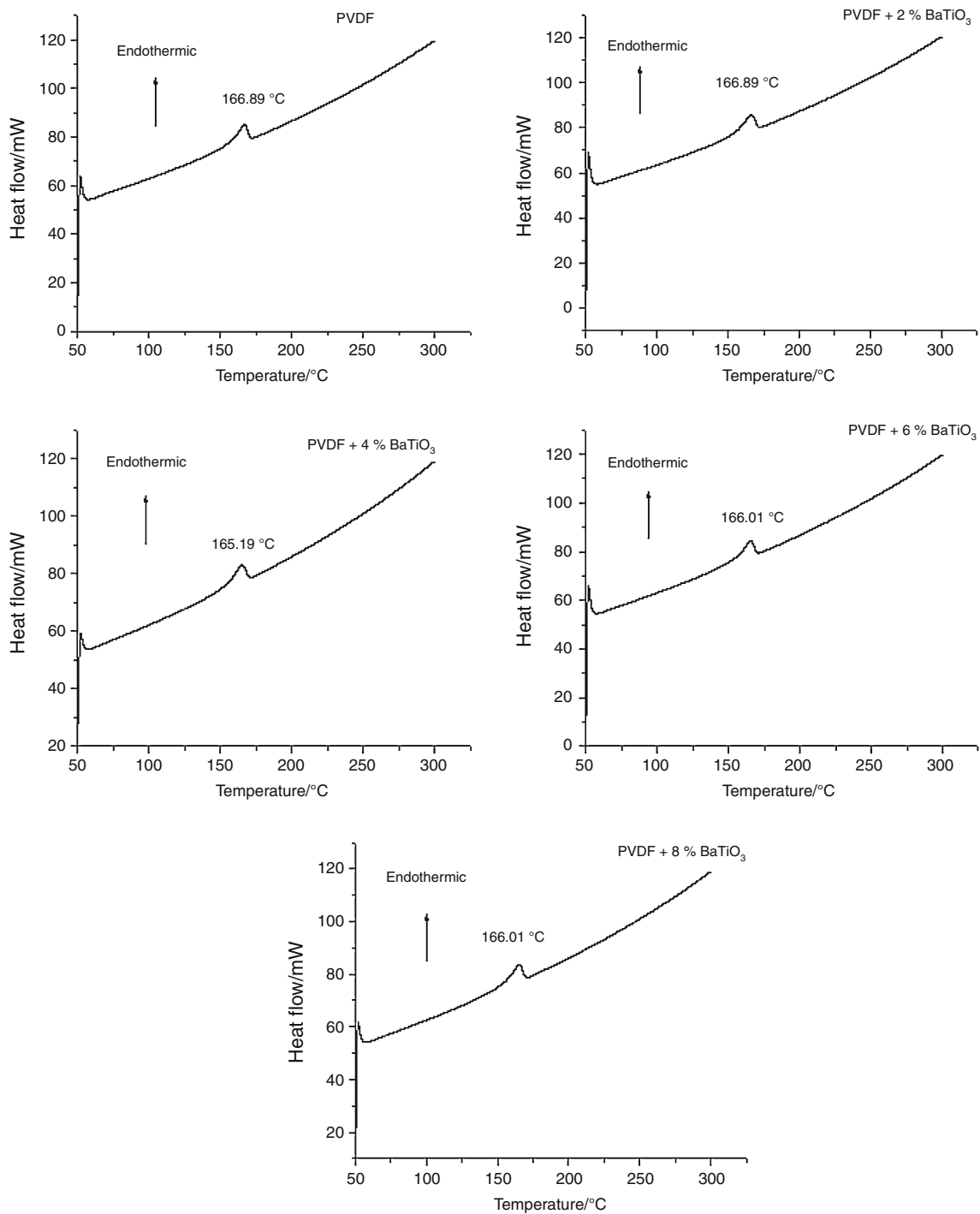


Fig. 5 DSC spectra of β phase PVDF and PVDF + BaTiO₃ nanocomposites

of BaTiO₃. Similar decreasing behaviors of the percentage crystallinity have been reported in our earlier work [20].

SEM and optical micrograph

Figure 2a–e show the SEM of Pristine β -phase PVDF and β -phase PVDF–BaTiO₃ with different mass% (2, 4, 6 and

8 mass%) of nanoparticles. Scanning electron micrographs show uniform dispersion of BaTiO₃ within β -phase PVDF. BaTiO₃ nanofillers have been imbedded in the pores available in the polymer matrix as shown in SEM images. Whiteness of the images increases with increase in loading concentration. Figure 3 shows the optical micrographs of pristine PVDF and PVDF/BaTiO₃ nanocomposite. The

crystalline morphology for PVDF observed spherulites (i.e., Fig. 3a, b). The similar patterns of spherulites in PVDF have been reported in the literature [37, 38]. The size of spherulites can be controlled by nucleation, cooling rate, and can vary from micrometer to centimeter [39].

In Fig. 3a the size and shape of the spherulites are almost homogeneous and arrange in regular manner due to semi crystalline nature of PVDF. Also spherulites represent the crystalline portion of the polymer. However, in Fig. 3b the size and shape of the spherulites are heterogeneous, somewhere small and somewhere large and arrange in irregular manner. This change in size of spherulites may be due to decreased in crystallinity or increased in amorphousity of PVDF. Therefore, BaTiO₃ play a nucleation role into nanocomposite of PVDF/BaTiO₃ by decreasing the crystallinity of PVDF. These results are supported by XRD data.

FTIR spectroscopy

Figure 4 shows the FTIR spectra of pristine and nanocomposites samples at various contents of BaTiO₃. The vibration modes of chemical bonds are characterized by the absorption bands of FTIR spectra. The various absorption bands in pristine and nanocomposite samples are assigned and summarized in Table 1. The FTIR spectra of the nanocomposite samples do not show any major change in bands, except some broadening and an increase/decrease in the intensity of bands have observed. Some weak bands present in pristine PVDF disappear at higher contents of BaTiO₃ but at wave number of 1664.16 and 1748.43 cm⁻¹, bonds are become strong with content of BaTiO₃ as compare to pristine sample. Further β -phase of PVDF is confirmed by the bond position at wave number 836.45 cm⁻¹ by FTIR which is originating due to the CH₂ group [34].

Thermal analysis

DSC

DSC measurement is the advancement of DTA analysis in which we have investigate the thermal degradation temperature of polymeric samples, whereas the DSC analysis shows the increasing or decreasing nature of polymeric samples. Figure 5 shows the DSC of β -phase PVDF and nanocomposites with different mass% of BaTiO₃. DSC spectra are not showing the glass transition temperature (T_g) in β -phase PVDF and in nanocomposites samples because β -phase PVDF nanocomposites result shows the glass transition temperature in the negative range of temperature as reported in the literature [40], but DSC spectra is showing the small peaks at 166.89, 166.89, 165.19, 166.01, 166.01 °C at pristine, 2, 4, 6, and 8 mass% of

BaTiO₃ in PVDF matrix. These peaks are melting temperature peaks, which are verifying with DTA result of β -phase PVDF–BaTiO₃ nanocomposites, XRD and DTA result as shown in Fig. 6 are also showing almost the same behavior of polymer nanocomposites with increasing concentration of nanofillers. DSC spectra show that melting point is not much more affected by loading of BaTiO₃ nanofillers in β -phase PVDF matrix.

Thermally stimulated discharge current (TSDC)

There are considerable interests in the TSDC of PVDF and PVDF–BaTiO₃ nanocomposites because of its use in piezoelectric and pyroelectric polymers. The dependence of the piezoelectric properties of PVDF and PVDF nanocomposites on the poling conditions, thus, one has to optimize the poling condition. TSDC might help to achieve this goal.

In semicrystalline polymers having a friction of the amorphous phase partially confined within the crystalline lamellae, as it is clear from microstructure of PVDF and PVDF–BaTiO₃ nanocomposites (Fig. 3a, b). Therefore, chain will have the constrained mobility and we may expect the serious changes in glass transition dynamics. Adam–Gibbs develops a theory by introducing the concept of cooperatively rearranging region that defines the smallest region around a relaxing unit [41]. Due to this unit, the transition will undergo around this small region. This region is order of nanometer, therefore, if chain in amorphous regions is constrained within geometric below such sizes, they are incapable to relax with the same characteristic times as the unconstrained chain, and will exhibit higher T_g values. In our earlier [40] publication, this

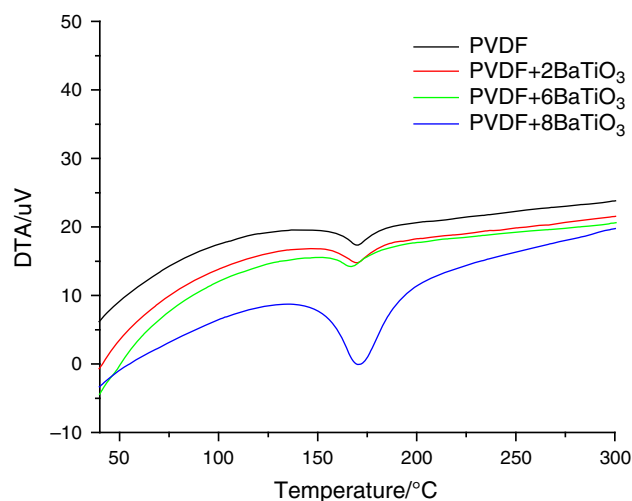


Fig. 6 DTA spectra of β phase PVDF and PVDF + BaTiO₃ nanocomposites

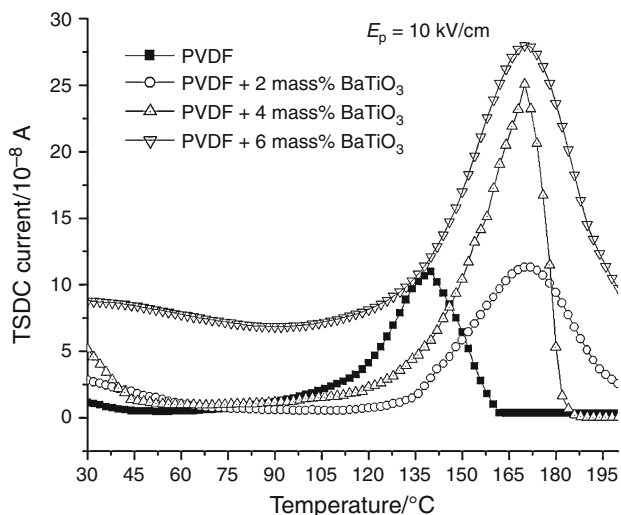


Fig. 7 TSDC spectra of β phase PVDF and PVDF + BaTiO₃ nanocomposites at polarizing field of 10 kV/cm

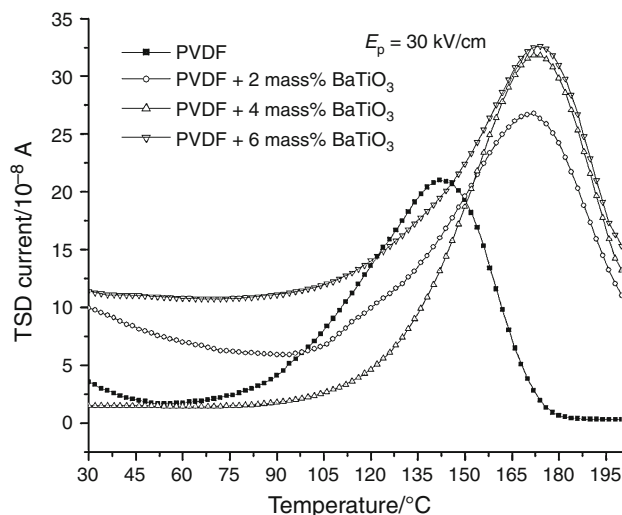


Fig. 9 TSDC spectra of β phase PVDF and PVDF + BaTiO₃ nanocomposites at polarizing field of 30 kV/cm

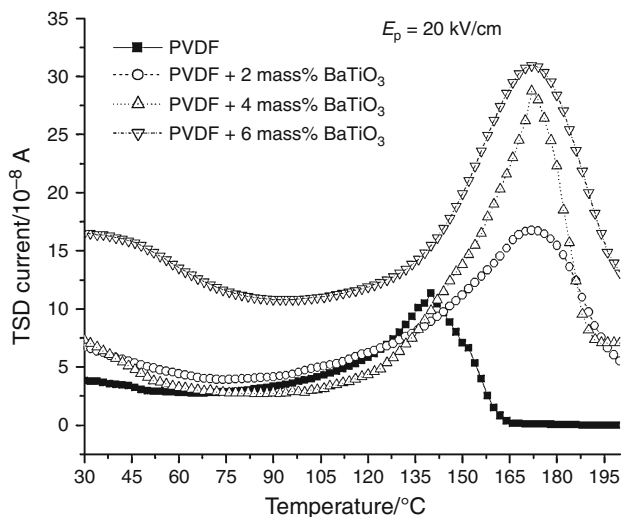


Fig. 8 TSDC spectra of β phase PVDF and PVDF + BaTiO₃ nanocomposites at polarizing field of 20 kV/cm

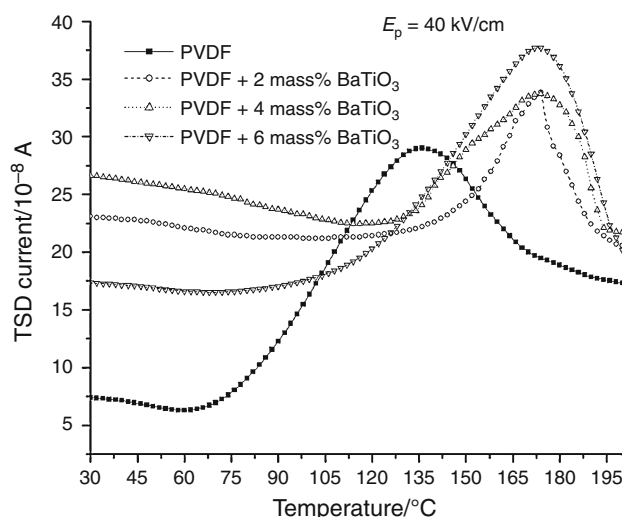


Fig. 10 TSDC spectra of β phase PVDF and PVDF + BaTiO₃ nanocomposites at polarizing field of 40 kV/cm

situation is achieved due to incorporation of ZnO nanoparticle in PVDF. The confinements imposed nanoparticles by varying the size of crystalline lamellae are enough to affect the segmental dynamics in polymers. The local motion of charge carrier will also be affected by size of lamellae. Hence, the confinement is imposed by the nanofillers of definite size is very important to understand relaxation mechanism in semicrystalline polymers like PVDF. The existence of nanofillers in matrix of semicrystalline polymers may introduce new relaxation process appears at high temperature quite above the glass transition temperature. In PVDF, the conformational mobility of the chains of the amorphous phase is significantly limited near the crystallites. This means that the relaxation process in

PVDF and PVDF–BaTiO₃ nanocomposites depend on the crystalline fraction and also on microstructure.

The existence of interfacial regions with properties lying those of crystalline and undisturbed amorphous regions has been revealed by percentage crystallinity. XRD result shows that % crystallinity of PVDF decreases with increase in BaTiO₃ nanoparticle contents. This evidence was demonstrated by SEM. The SEM images clearly demonstrate the existence of interface between amorphous and crystalline region. SEM also represents that the BaTiO₃ nanoparticles are encapsulated between amorphous and crystalline boundaries.

In general, the TSDC of PVDF is characterized by two peaks one at -42°C corresponding to glass rubber

Table 2 TSDC parameters of PVDF–BaTiO₃ thermo-nanoelectrets

Thermo-nanoelectrets	Polling temp/K	Polling field/kV cm ⁻¹	Peak position/K	Peak current 10 ⁻⁸ /A	Activation energy/eV	Charge release 10 ⁻⁹ /C	Relaxation time/s
PVDF	303	10	413	10.97	0.40	5.48	8.34E–12
		20	413	11.33	0.43	7.40	19.14E–12
		30	415	21	0.76	20.16	1.74E–7
		40	417	39.73	1.06	37.90	6.90E–4
PVDF + 2 mass% BaTiO ₃		10	443	11.29	0.55	8.67	2.08E–10
		20	445	16.76	0.66	18.02	3.33E–9
		30	445	26.8	0.87	30.87	8.78E–7
		40	447	33.83	1.28	45.46	3.09E–14
PVDF + 4 mass% BaTiO ₃		10	443	25.06	0.73	11.54	1.94E–8
		20	445	28.73	0.87	18.75	7.48E–7
		30	445	31.82	1.34	30.54	1.68E–1
		40	447	33.68	1.53	53.02	1.84E+1
PVDF + 6 mass% BaTiO ₃		10	443	27.99	0.91	24.72	2.76E–6
		20	445	30.96	1.18	32.10	2.88E–3
		30	447	32.59	1.54	42.55	2.77E+1
		40	447	37.69	1.67	63.68	7.41E+2

transition attributed by dipolar relaxation in amorphous phase. However, second peak at 140–180 °C is probably due to dipolar relaxation in the crystalline phase or in the region intermediate between crystalline and amorphous phases. Since this peak appeared well above glass transition temperature, therefore, destruction of charges accumulated near the amorphous–crystalline boundaries (Maxwell–Wagner effect) is also responsible for this peak. Figures 7, 8, 9 and 10 show a peak and, therefore, it involves the undistributed polarization. The PVDF nanocomposites are heterogeneous system consisting of different components or phases. These components have different dielectric constants and conductivities, electric charges are accumulated near the interface, when sample heated and subjected to a field. These charges are frozen in the interface if the field is maintained during cooling. During TSDC run, the interfacial charges are destroyed, because local field in the dissimilar parts of the sample is reversed so that neutralizing charges of opposite sign are conveyed to the interface. This process of giving rise to a peak is known as interfacial relaxation peak caused by Maxwell–Wagner effect. This peak is only expected in semicrystalline or micro and nanocomposite material as observed in present study. The activation energy of this peak is increasing with increase of polarizing field (i.e., Table 2). The volume friction of nanoparticles increases the current TSD as shown in Figs. 7, 8, 9 and 10. This is similar to increase of piezoelectric coefficient. The similar behavior of increase of piezoelectric coefficient is

demonstrated in the literature [42]. The piezoelectric coefficient is observed to be increased with BaTiO₃ contents; for PVDF pristine, its value was 37.8, but for PVDF/BaTiO₃ its values are lying between 48.3 and 53.1. This increase of current TSD demonstrates the higher polarizability of PVDF. The relaxation time, charge storage, and activation energy are significantly affected by volume friction of BaTiO₃ in PVDF matrix.

Another fact supporting to this peak is the activation energy. The activation energy value lies between 0.40 and 1.67 eV, is evidence for traps are energetically distributed in the bulk of polymer. The higher value of activation energy supporting the view that TSDC peak arises from space charge motion [40]. High temperature peak in PVDF is also altered drastically by impurities, fillers, absorbed water, and swelling agents. The fillers clearly increase the charge storage as shown in Table 2. This may be probable due to their dissociation or promote dissociation. It is observed that from Figs. 7, 8, 9 and 10 the position of peak is almost same and its height being affected because of low temperature polarization of all samples. The structure of polymer nanocomposite is complicated, therefore, it is very difficult to distinguish several relaxation processes and no any theory is being developed for TSDC of nanocomposites. However, appearance of single peak in TSDC experiment shows that the single relaxation process is the possible mechanism of these results. Activation energy corresponding to TSDC peak refers that the dipolar and interfacial polarizations are merged together and produce the single peak.

Conclusions

β -phase PVDF and BaTiO₃ filled polymer nanocomposites film have been prepared successfully. SEM images supported the uniform dispersion of nanoparticles in the bulk of polymer using very simple technique of sample preparation. The XRD spectra analyzed that BaTiO₃ reduces the crystallinity of polymer. The effect of BaTiO₃ nanoparticle on thermal degradation is significantly affected, however, melting point of β -phase PVDF is remains almost same. It is concluded from FTIR interferometry that the BaTiO₃ is chemically non-interacting nature with PVDF molecules; therefore, the interaction of BaTiO₃ is van der waals type of weak interaction with β -phase PVDF. It is further concluded that the weak interaction of BaTiO₃ is the origin of significant variation of crystallinity and thermal degradation.

It could be understand by DSC, DTA, and TSDC techniques that TSDC peak (i.e., depolarization peak) of nanocomposite material is similar to decomposition peak as observed by DSC and DTA. Therefore, TSDC measurement is not only limited to study the charge storage, charge transport, and charge relaxation phenomenon in material but also applied to study thermal properties by means of glass transition temperature, melting temperature, and polymorphism. Further, increase in depolarization current according to increase in concentration of BaTiO₃ in PVDF matrix is an agreement with increasing value of d_{33} coefficients.

Acknowledgements The authors are thankful to Science and Engineering Research Board (SERB), DST, New Delhi (India) (letter no. SR/S2/CMP-0091/2010) for providing financial support. The authors are also thankful to Director, AIRF-JNU New Delhi 377, (India) for providing FTIR, SEM, and XRD characterization facilities. The technical advice of Prof. Ranjit Singh is highly solicited. The facilities provided by Director, Hindustan College of Science and Technology are gratefully acknowledged.

References

- Nathani H, Dasari A, Misra RDK. On the reduced susceptibility to stress whitening behavior of melt intercalated polybutene–clay nanocomposites during tensile straining. *Acta Mater.* 2004;52:3217–27.
- Hadal R, Yuan Q, Jog JP, Misra RDK. On stress whitening during surface deformation in clay-containing polymer nanocomposites: a microstructural approach. *Mater Sci Eng A.* 2006;A418:268–81.
- Kornmann X, Lindberg H, Berglund LA. Synthesis of epoxy–clay nanocomposites: influence of the nature of the clay on the structure. *Polymer.* 2001;42:1303–10.
- Chiang CK, Popielarz R. Polymer composites with high dielectric constant. *Ferroelectrics.* 2002;275:1–9.
- Hilczner B, Kulek J, Markiewicz E, Kosec M, Malic B. Dielectric relaxation in ferroelectric PZT–PVDF nanocomposites. *J Non Cryst Solids.* 2002;5:167–73.
- Ishida H, Campbell S, Blackwell J. General approach to polymer nanocomposite preparation. *Chem Mater.* 2000;12:1260–7.
- Kontos GA, Soulintzis AL, Karahaliou PK, Psarras GC, Georga SN, Krontiras CA, Pisanias MN. Electrical relaxation dynamics in TiO₂-polymer matrix composites. *Express Polym Lett.* 2007;1:781–9.
- Kowbel W, Xia X, Withersa JC, Crocker MJ, Wada BK. PZT/PVDF flexible composites for actuator and sensor applications. *SPIE.* 1998;3324.
- Boria FJ, Bachmann RJ, Ifju PG, Quinn RD, Vaidyanathan R, Perry C, Wagener J. A sensor platform capable of aerial and terrestrial locomotion. *Intelligent robots and systems (IROS) Alberta.* 2005;August:2–6.
- Pawlowski KJ, Belvin HL, Raney DL, Su J, Harrison JS, Siochi EJ. Electrospinning of a micro-air vehicle wing skin. *Polymer.* 2003;44:1309–14.
- Chronakis IS. Novel nanocomposites and nanoceramics based on polymer nanofibers using electrospinning process—a review. *J Mater Process Technol.* 2005;167:283–93.
- Sigmund W, Yuh J, Park H, Maneeratana V, Pyrgiotakis G, Daga A, Taylor J, Nino JC. Processing and structure relationships in electrospinning of ceramic fiber systems. *J Am Ceram Soc.* 2006;89:395–407.
- Wang Y, Aponte M, Leon N, Ramos I, Furlan R, Pinto N. Synthesis and characterization of ultra-fine tin oxide fibers using electrospinning. *J Am Ceram Soc.* 2005;88:2059–63.
- Yordem OS, Gülleroğlu M, Ögut E, Menciloglu YZ, Papila M. Piezoelectric polymer and ceramic ultrafine fibers for piezocomposite films. In: *Proceedings of the American Society for Composites, 21st Technical Conference, Dearborn.* 2006; September:17–20.
- Gregorio R Jr, Ueno EM. Effect of crystalline phase, orientation and temperature on the dielectric properties of poly (vinylidene fluoride) (PVDF). *J Mater Sci.* 1999;34:4489–500.
- Pramoda KP, Mohamed A, Phang IY, Liu T. Crystal transformation and thermo mechanical properties of poly (vinylidene fluoride)/clay nanocomposites. *Polym Int.* 2005;54:226–32.
- Gregorio R Jr, Cestari M. Effect of crystallization temperature on the crystalline phase content and morphology of poly (vinylidene fluoride). *J Polym Sci Part B.* 1994;32:859–70.
- Dzenis Y, Feng R, Larsen G, Turner J, Zeng X. Manufacturing of novel continuous nanocrystalline ceramic nanofibers with superior mechanical properties. *NSF Nanoscale Science and Engineering Grantees Conference 2003.* Arlington.
- Stroyan JJ. Processing and Characterization of PVDF, PVDF–TrFE, and PVDF–TrFE–PZT composites. *Washington State University, Washington;*2004.
- Gaur MS, Singh PK, Suruchi, Chauhan RS. Structural and thermal properties of polysulfone–ZnO nanocomposites. *J Therm Anal Calorim.* 2012; doi:10.1007/s10973-012-2357-8.
- Cui C, Baughman RH, Iqbal Z, Kazmar TR, Dahlstrom DK. Improved piezoelectric 0-3 ceramic particle/polymer composites. *Ferroelectrics.* 1996;2:605–8.
- Sessler GM. *Electrets., Topics in applied physics* Springer-Verlag: Heidelberg; 1980. p. 33.
- Sangawar VS, Chikhalikar PS, Dhokne RJ, Ubale AU, Meshram SD. Thermally stimulated discharge conductivity in polymer composite thin films. *Bull Mater Sci.* 2006;29:413–6.
- Sealssuer DA. Electrical conduction in polymers. In: *Sear DA, editor. Electrical properties of polymers.* New York: Academic Press; 1982. p. 1–58.
- Tripathi A, Tripathi AK, Pillai PKC. Thermo-electret state in PVC-PE poly blends. *J Appl Phys.* 1988;64:2031–3.
- Mekishev GA et al. AIP Conference Proceeding, 2009; 1203. p. 568–573.
- Pillai PKC, Narula GK, Tripathi AK, Mendiratta RG. Thermally stimulated discharge current studies in polarized polypropylene. *Physica Status Solidi (a).* 1981;67:649–54.

28. Verma A, Tripathi AK, Chariar V, Goel TC, Pillai PKC. Thermally stimulated discharge current studies in a polymethyl methacrylate–polystyrene blend. In: Proceedings of 8th International Symposium on Electrets (ISE-8), Paris; 1994. p. 540–5.
29. Burghate DK, Deogaonkar VS, Sawarkar SB, Yawale SP, Pakade SV. Thermally stimulated discharge current (TSDC) and dielectric constant of semiconducting glasses. *Bull Mater Sci.* 2003; 26:267–71.
30. Dang ZM, Wang HY, Zhang YH, Qi JQ. Morphology and dielectric property of homogenous BaTiO₃/PVDF nanocomposites prepared via the natural adsorption action of nanosized BaTiO₃. *Mol Rapid Commun.* 2005;26:1185–9.
31. Sekar R, Tripathi AK, Pillai PKC. X-ray diffraction and dielectric studies of a BaTiO₃: PVDF composite. *Mater Sci Eng B.* 1989;5:33–6.
32. Hasegawa R, Takahashi Y, Chatani Y, Tadakoro. Crystal structures of three crystalline forms of poly (vinylidene fluoride). *Polym J.* 1972;2:600–10.
33. Wang TT, Herbert JM, Glass AM. The applications of ferroelectric polymer. New York: Blackie; 1988.
34. Tae KJ. Nanoscale characterization of solution-cast poly (vinylidene fluoride) thinfilms using atomic force microscopy. Texas: A&M University; 2005.
35. Gaur MS, Singh PK, Chauhan RS. Optical and thermo electrical properties of ZnO nano particle filled polystyrene. *J Appl Polym Sci.* 2010;118:2833–40.
36. Hussain AMP, Kumar A, Singh F, Avasthi DK. Effects of 160 MeV Ni¹²⁺ ion irradiation on HCl doped polyaniline electrode. *J Phys D Appl Phys.* 2006;39:750.
37. Toda A, Arita T, Hikosaka M. Three-dimensional morphology of PVDF single crystals forming banded spherulites. *J Polym.* 2001;42:2223–33.
38. Chiu HJ, Huang JM, Don TM. Spherulitic morphology and crystallization kinetics of melt-miscible blends of poly (vinylidene fluoride) with poly (3-hydroxybutyrate). *Tamkang J Sci Eng.* 2008;11:201–9.
39. Vasile C. Handbook of polyolefins. Boca Raton: CRC Press; 2000. p. 183.
40. Indolia AP, Gaur MS. Investigation of structural and thermal characteristics of PVDF/ZnO nanocomposites. *J Therm Anal Calorim.* 2012;. doi:10.1007/s10973-012-2834-0.
41. Adms G, Gibbs JH. On temperature dependence of cooperative relaxation properties in glass forming liquids. *J Chem Phys.* 1965;43:139–46.
42. Perlmann MM. Electrets, charge storage and transport in dielectrics. Princeton: Electrochemical society; 1973. p. 128–40.